ON NEAR-WALL HOT-WIRE MEASUREMENTS

Y. T. Chew, B. C. Khoo and C. J. Teo
Department of Mechanical & Production Engineering
National University of Singapore
Kent Ridge, Singapore 119260

1. INTRODUCTION

During the past decade, the quest for drag reduction has prompted numerous researchers to propose various passive skin-friction reduction schemes which seek to alter the flow structures and velocity profile very close to the wall. Examples of such schemes include the employment of riblets, large eddy break-up (LEBU) devices, compliant surfaces and polymers. Near-wall velocity measurements are hence imperative in assessing the merits of these passive drag reduction schemes, so that detailed comparison can be made with respect to the unmanipulated flow in order that the physics and mechanisms responsible for the said reduction in drag can be brought to light. A further application of near-wall velocity measurement arises from its application to near-wall turbulence modeling. The two-equation k-ε model which attempts to model most of the constituent terms in the transport equations for k (turbulence kinetic energy) and ε (dissipation rate of the turbulence kinetic energy), has been and may continue to be a turbulence model which is extensively used by many computational fluid dynamists. At low Reynolds numbers, wall damping functions are invariably applied to ensure that the viscous stresses take over from the Reynolds stresses in the viscous sublayer adjacent to the wall. However, the damping functions introduced to model the different terms in the ε-equation are rather ad-hoc. Near-wall measurements can thus serve as a means for computational fluid dynamists to propose more accurate turbulence models in the near-wall region and to check the validity of their computational results near the wall.

The rapid advancement of PIV and the accessibility of LDV have not resulted in the demise of the use of hot-wire anemometry, especially for near-wall measurements. Both the LDV and PIV require seeding of the flow and measurements significantly depend on the passage of the said particles through the respective control volumes, hence yielding a non-continuous output. This issue is accentuated in the near-wall region where the particle count diminishes considerably, resulting in an appreciably lower and variable data rate. Moreover, the relatively large measuring volume of the LDA gives rise to uncertainties pertaining to the spatial averaging of the particle velocity, especially in the near wall region where the velocity gradient is normally large. In addition, most near-wall LDA measurements available in the literature are limited to low Reynolds numbers. The hot-wire anemometer's smallness in size and its ability to track fluctuating velocities with a high degree of responsiveness establishes it as a primary means for continuous turbulent velocity measurements, even at high Reynolds numbers. However, a hot wire calibrated under free stream conditions suffers from influence of wall effects. The recent works of Chew et al (1994) and Khoo et al (1996) have proposed and verified various calibration procedures for the use of marginally-elevated hot wires to obtain accurate time-resolved velocity field. Khoo et al (1998) further quantified the dynamic frequency response of a near-wall hot wire, which is typically O(2 kHz) for $y^+ \leq 5$. These investigations help to establish and provide the basis for the continual application of hot-wire anemometry for near-wall turbulence measurements.

2. RESULTS AND DISCUSSION

Velocity measurements were carried out in both a fully developed turbulent channel flow at $h^+ = 180$ and 390 ($h^+ \equiv hu_\tau/\nu$, where h is the half channel height and u_τ is the friction velocity at the wall) and flat plate boundary layer flow at Re_θ (based on the momentum thickness) of 2900, 3400 and 4100 using near-wall hot-wire probes. Construction of the near-wall hot-wire probe, the channel

and the wind tunnel facilities where measurements were obtained are available in Khoo et al (1996, 1998) and interested readers may refer to them for further details. The wall shear stress and hence the friction velocity for the channel flow were determined from the constant streamwise pressure gradient measured via pressure tappings spaced along the length of the channel. For the boundary layer flow, the Clauser chart technique was employed to determine the friction velocity. The near-wall hot-wire probe was calibrated using a similar laminar flow calibration rig, used previously in Khoo et al (1998) and Chew et al (1998) to study the dynamic frequency response of near-wall and flush-mounted hot-wire and hot-film probes respectively. The rig consists of a flat, upper rotating perspex disk of diameter 300 mm and a flat bottom stationary disk of identical size and material. A laminar, near-Couette flow is set up in the gap between the two disks when the top disk is set into rotation, thus imposing a known azimuthal velocity (U) on the hot wire for correlation to the anemometer's output voltage (E) via King's law.

Figure 1 shows results of the streamwise intensity of turbulence in the viscous sublayer of the turbulent channel flow and flat plate boundary layer flow. The DNS results of Antonia et al (1991) for a fully developed turbulent channel flow at h^+ = 180 and 395 have also been included for purpose of comparison. The experimental results for the channel flow compare favorably with the computational results. In particular, for the same value of y^+, an increase in h^+ results in a corresponding increase in the streamwise turbulence intensity in the viscous sublayer. The values obtained for the boundary layer at different Re_θ concur well with those for the channel flow at h^+ = 390. Figure 2 shows results for the spanwise intensity of turbulence obtained using an inclined hot wire utilizing an 'effective angle' method, originally proposed by Bradshaw (1971). Low Reynolds number effects are again evident for the channel flow, as manifested by the monotonic increase in the spanwise turbulence intensity when h^+ is increased. In contrast to the streamwise turbulence intensity which remains fairly constant in the viscous sublayer, the spanwise intensity exhibits a more rapid decline with increasing values of y^+.

Kim et al's (1987) DNS results for a channel flow at h^+ = 180 show that the rms value of the normal component of the velocity fluctuations near the wall can be correlated using $v'^+ = 0.009y^{+2}$, with v'/u' being at most 7 % at $y^+ \approx 5$ and decreasing rapidly as $y^+ \rightarrow 0$. Gunther et al (1998) obtained a rather similar expression $v' = 0.012y^{+2}$ as $y^+ \rightarrow 0$ for their DNS of a channel flow at h^+ = 300, with v'/u' attaining a value of 8 % at $y^+ \approx 5$. Since the normal component of the fluctuating velocity in the viscous sublayer is small and can therefore be neglected, the turbulence kinetic energy k (conventionally defined as $0.5[u'^2 + v'^2 + w'^2]$) is evaluated using the mean square values of the streamwise and spanwise velocity fluctuations. The variation of k^+ (normalized using u_τ) in the viscous sublayer is presented in Fig. 3. It is apparent that with the exception of the results for the channel flow at h^+ =180, the values of k^+ in the viscous sublayer can be correlated well by

$$k^+ = -0.0059y^{+3} + 0.1081y^{+2}. \qquad (1)$$

This correlation should be invaluable to users of the k-ε model in modeling the behavior of k in the viscous sublayer.

The full expression for the dissipation rate ε is given by

$$\varepsilon = \nu\overline{u_{i,j}(u_{i,j} + u_{j,i})}, \qquad (2)$$

where $u_{i,j}$ represents the velocity derivative $\partial u_i/\partial x_j$. However, it should be noted that it is virtually impossible to measure all the 12 terms which appear on the right hand side, especially in the near-wall region where wall influence increasingly dominates generally for all velocity-measuring instruments, particularly the hot wire. The physical presence of the wall also causes problems in maneuvering the instrument to obtain a fine distribution across the usually thin viscous sublayer. By assuming the dissipating range of eddy sizes to be statistically isotropic, the dissipation rate ε_{iso} can be substantially simplified to

$$\varepsilon_{iso} = 15\nu\overline{(\frac{\partial u}{\partial x})^2}. \qquad (3)$$

By further assuming the validity of Taylor's hypothesis, equation (3) becomes

$$\varepsilon_{iso} = 15\frac{\nu}{U_c^2}\overline{(\frac{\partial u}{\partial t})^2}, \qquad (4)$$

where U_c is the local convection velocity, which is usually assumed to be equal to the mean velocity $\overline{U}$ at the point of measurement. Furthermore, if $E_u(k_1)$ is the spectral density of longitudinal velocity fluctuations, where the wavenumber $k_1 = 2\pi f/U_c$,

$$\varepsilon_{iso} = 15\nu\int_0^\infty k_1^2 E_u(k_1)dk_1. \qquad (5)$$

Equations (4) and (5) are two commonly used methods for estimating ε. Azad & Kassab (1989) employed hot wires of different lengths and diameters and obtained ε_{iso} using equations (4) and (5). For wires with the same length and diameter, Azad & Kassab found that the spectra (i.e. equation (5)) yielded results of ε_{iso} that were consistently higher than those obtained using $\overline{(\partial u/\partial t)^2}$ (i.e. equation (4)) by about 30%. Their measurements were made in the wall-remote region of $y^+ \gtrsim 50$. We applied both methods of evaluating ε_{iso} to the channel and boundary layer flows for the wall-remote region as carried out in Azad & Kassab and the near-wall region. The spectral density $E_u(k_1)$ of longitudinal velocity fluctuations was obtained using a Fast Fourier Transform (FFT) algorithm, and the convective velocity U_c was also assumed to be the mean velocity $\overline{U}$ at the point of measurement. Contrary to the findings of Azad

& Kassab, at the same value of y^+ for a particular flow, both methods of evaluating ε_{iso} yield almost identical results, even in the very near-wall viscous sublayer and buffer region. Elsner et al (1993) also found that both methods yielded almost identical values for ε_{iso} from their measurements conducted in a turbulent channel flow. Strictly speaking, the assumption that the convective velocity U_c is equal to the mean velocity $\overline{U}$ at the point of measurement when Taylor's hypothesis is invoked requires that the streamwise turbulence intensity be less than 15-20%, which is clearly violated in the buffer region and especially in the viscous sublayer, where the streamwise turbulence intensity registers values as high as 40%. Johansson et al (1991) analyzed the DNS results of Kim et al (1987) for a channel flow at $h^+ = 180$ using a VISA technique (the spatial counterpart of the VITA technique) and deduced that the propagation velocity of the near-wall shear layers was $10.6u_\tau \pm 1.0u_\tau$. Following the methodology of Kim et al, Xu et al (1996) conducted a DNS of a channel flow at $h^+ = 172$ to analyze the origin of high kurtosis levels of the normal velocity fluctuations in the viscous sublayer. Xu et al observed that the high values of the kurtosis were due to extremely rare spatial and temporal events characterized by spikes in the time series with extremely negative values. These spikes only appeared in the very near-wall region and were propagated at a velocity of $10.6u_\tau \pm 0.8u_\tau$, which is strikingly close to the value deduced by Johansson et al. It is interesting to note that the propagation velocity of shear layers, pressure fluctuations and spikes in the viscous sublayer ($\sim 10.6u_\tau$) is larger than the local mean velocity, this difference increasing as the wall is approached. Denoting $(\varepsilon_{iso})_1$ as the value of ε_{iso} evaluated by assuming the convective velocity U_c in equation (4) to be $10.6u_\tau$, the distributions of $(\varepsilon_{iso}^+)_1$ [$\equiv (\varepsilon_{iso})_1\nu/u_\tau^4$)] in the viscous sublayer for the channel and boundary layer flows are plotted in Fig. 4 together with the channel flow DNS results[1] of Kim et al (1987) for $h^+ = 180$ and Antonia et al (1991) for $h^+ = 395$. It can be seen that for both values of h^+, within the viscous sublayer, agreement between the experimental values of $(\varepsilon_{iso}^+)_1$ and the DNS results is good, thus vindicating the accuracy of our hot-wire measurements in the very near-wall region. As h^+ increases from 180 to 390, the experimental value of $(\varepsilon_{iso}^+)_1$ at the same y^+ increases, thus reflecting the presence of low Reynolds number effects, which is consistent with the trend borne out by the other turbulence statistics.

3. REFERENCES

Antonia R. A., Kim J. & Browne L. W. B.: Some characteristics of small-scale turbulence in a turbulent duct flow. *J. Fluid Mech.* 233, 369-388, 1991.

Azad R. S. & Kassab S. Z. 1989: A new method of obtaining dissipation. *Exps. Fluids* 7, 81-87.

Bradshaw P. 1971: *An Introduction to Turbulence and its Measurement*, Pergamon Press.

Chew Y. T., Khoo B. C. & Li G. L. 1994: A time-resolved hot-wire shear stress probe for turbulent flow: use of laminar flow calibration. *Exps. Fluids* 17, 75-83.

Chew Y. T., Khoo B. C., Lim C. P. & Teo C. J.: Dynamic response of hot-wire anemometer. Part II: A flush-mounted hot-wire and hot-film probes for wall shear stress measurements. *Meas. Sci. Tech.* 9, 762-776.

Elsner J. W., Domagala P. & Elsner W. 1993: Effect of finite spatial resolution of hot-wire anemometry on measurements of turbulence energy dissipation. *Meas. Sci. Tech.* 4, 517-523.

Gunther A., Papavassiliou D. V., Warholic M. D. & Hanratty T. J. 1998: Turbulent flow in a channel at a low Reynolds number. *Exps. Fluids* 25, 503-511.

Johansson A.V., Alfredsson P. H. & Kim J. 1991: Evolution and dynamics of shear-layer structures in near-wall turbulence. *J. Fluid Mech.* 224, 579-599.

Khoo B. C., Chew Y. T. & Li G. L. 1995: A new method by which to determine the dynamic response of marginally elevated hot-wire anemometer probes for near-wall velocity and wall shear stress measurements. *Meas. Sci. Tech.* 6, 1399-1406.

Khoo B. C., Chew Y. T. & Li G. L. 1996: Time-resolved near-wall hot-wire measurements: use of laminar flow wall correction curve and near-wall calibration technique. *Meas. Sci. Tech.* 7, 564-575.

Khoo B. C., Chew Y. T., Lim C. P. & Teo C. J. 1998: Dynamic response of hot-wire anemometer. Part I: A marginally-elevated hot-wire probe for near-wall velocity measurements. *Meas. Sci. Tech.* 9, 749-761.

Kim J., Moin P. & Moser R. 1987: Turbulence statistics in fully developed channel flow at low Reynolds number. *J. Fluid Mech.* 177, 133-166.

Xu C., Zhang Z., den Toonder J. M. J. & Nieuwstadt F. T. M. 1996: Origin of high kurtosis levels in the viscous sublayer. Direct numerical simulation and experiment. *Phys. Fluids* 8, 1938-1944.

[1] The DNS results for ε_{iso} are obtained directly from equation (3) without invoking Taylor's hypothesis.

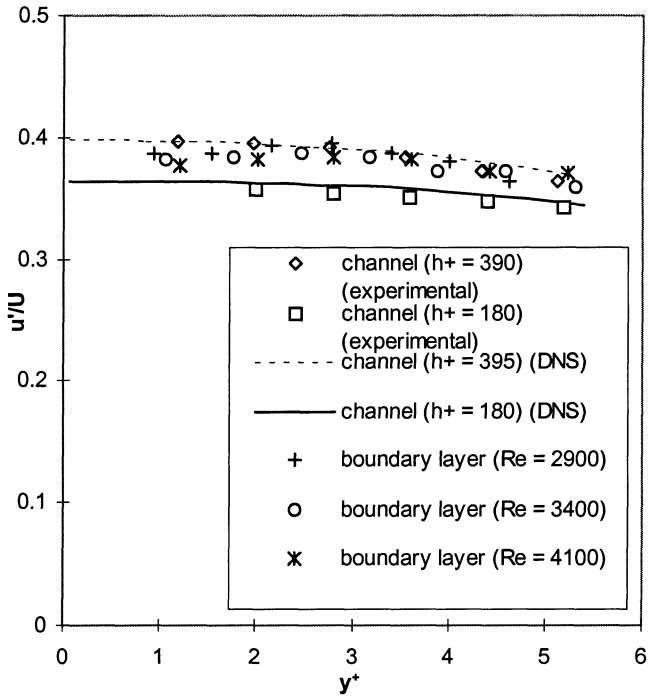

Fig. 1 Streamwise turbulence intensity distribution in the viscous sublayer.

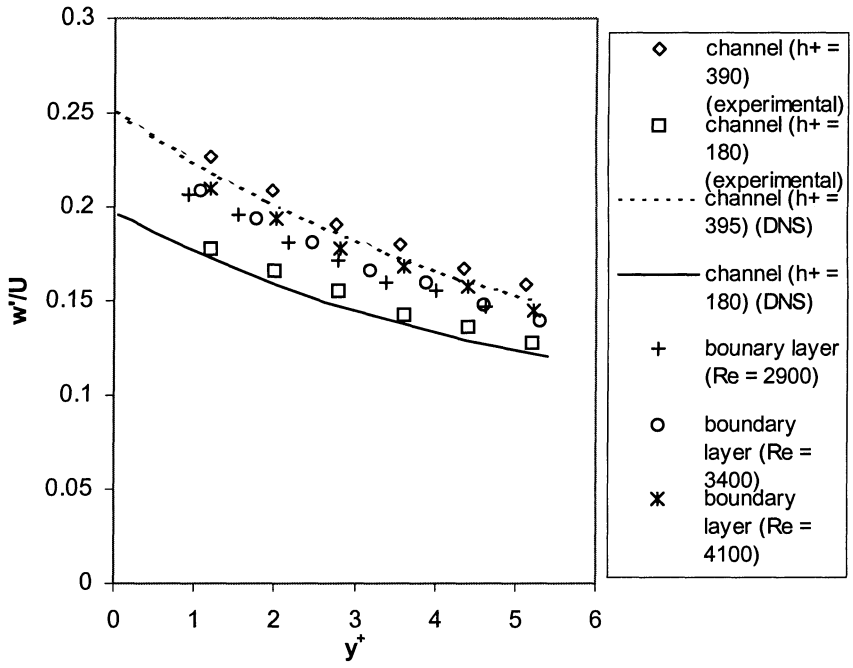

Fig. 2 Spanwise turbulence intensity in the viscous sublayer.

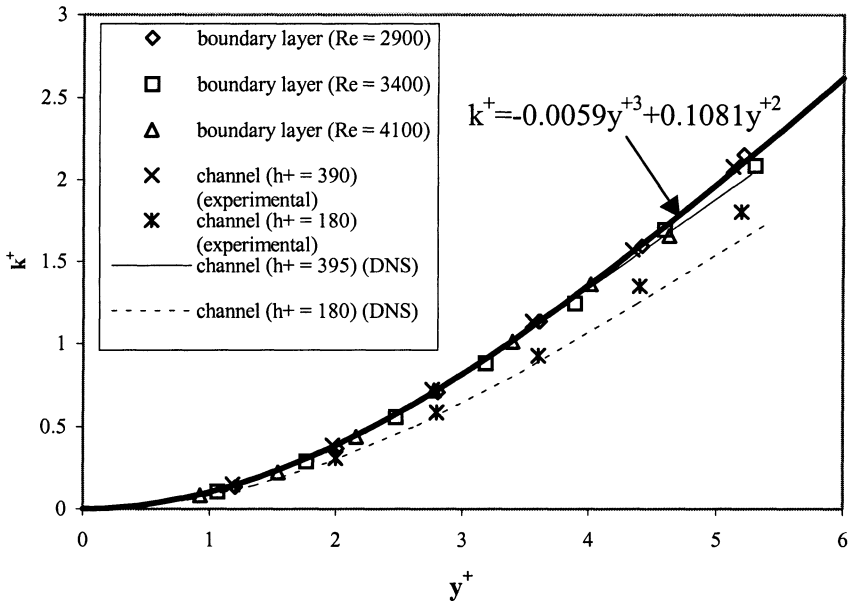

Fig. 3 Distribution of normalized turbulence kinetic energy k^+ in the viscous sublayer.

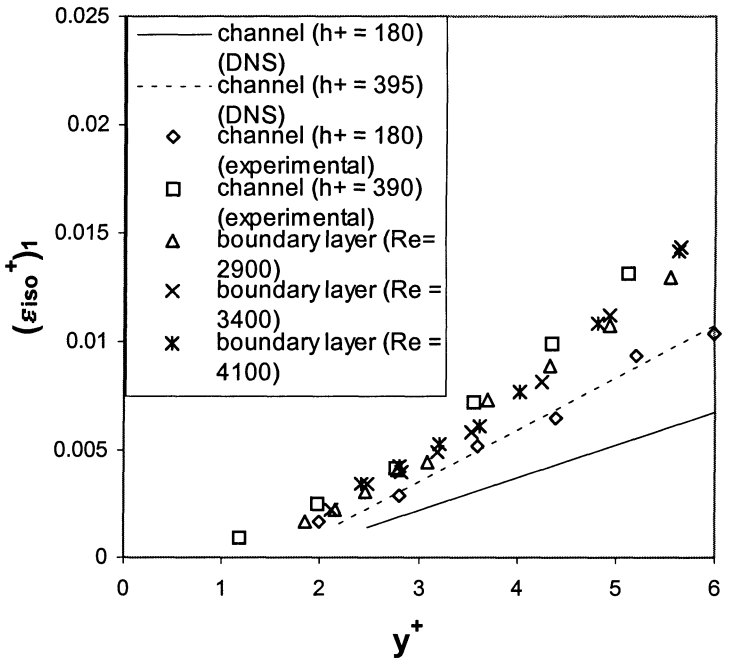

Fig. 4 Distribution of $(\varepsilon_{iso}^+)_1$ in the viscous sublayer.